

**A Comparison of the Particle Flow in Three-Jet and Radiative
Two-Jet Events from e^+e^- Annihilation at $E_{cm} = 29$ GeV***

P. D. Sheldon, G. H. Trilling, A. Petersen, G. Abrams, D. Amidei^(a), A. R. Baden,
T. Barklow, A. M. Boyarski, J. Boyer, P. R. Burchat^(b), D. L. Burke,
F. Butler, J. M. Dorfan, G. J. Feldman, G. Gidal, L. Gladney^(c), M. S. Gold,
G. Goldhaber, L. Golding^(d), J. Haggerty, G. Hanson, K. Hayes, D. Herrup,
R. J. Hollebeek^(c), W. R. Innes, J. A. Jaros, I. Juricic, J. A. Kadyk,
D. Karlen, A. J. Lankford, R. R. Larsen, B. W. LeClaire, M. Levi,
N. S. Lockyer^(c), V. Lüth, C. Matteuzzi^(e), M. E. Nelson^(f), R. A. Ong,
M. L. Perl, B. Richter, K. Riles, M. C. Ross, P. C. Rowson^(g), T. Schaad^(h),
H. Schellman^(a), W. B. Schmidke, C. de la Vaissiere⁽ⁱ⁾, D. R. Wood,
J. M. Yelton^(j), and C. Zaiser

*Lawrence Berkeley Laboratory and Department of Physics
University of California, Berkeley, California 94720*

*Stanford Linear Accelerator Center
Stanford University, Stanford, California 94305*

*Department of Physics
Harvard University, Cambridge, Massachusetts 02138*

Submitted to *Physical Review Letters*

* This work was supported in part by the U.S. Department of Energy under Contracts No. DE-AC03-76SF0098, No. DE-AC03-76SF00515, and No. DE-AC02-76ER03064.

- (a) Present address: University of Chicago, Chicago, IL 60637
- (b) Present address: University of California, Santa Cruz, CA 95064
- (c) Present address: University of Pennsylvania, Philadelphia, PA 19104
- (d) Present address: Therma-Wave, Inc., Fremont, CA 94539
- (e) Present address: CERN, CH-1211 Genève 23, Switzerland
- (f) Present address: California Institute of Technology, Pasadena, CA 91125
- (g) Present address: Columbia University, New York, NY 10027
- (h) Present address: Université de Genève, CH-1211, Genève 4, Switzerland
- (i) Present address: LPNHE, Université Pierre et Marie Curie, F-75230 Paris, France
- (j) Present address: Oxford University, Oxford, England

Abstract

We have made a detailed comparison of the charged particle flow in 3-jet events ($e^+e^- \rightarrow q\bar{q}g$) and radiative 2-jet events ($e^+e^- \rightarrow q\bar{q}\gamma$) from e^+e^- annihilation at $E_{cm} = 29$ GeV. Accurate comparisons can be made because these two event types have similar topologies. In the angular region between the quark and anti-quark jets, we observe substantially fewer charged tracks in the 3-jet events than in the radiative 2-jet events.

According to quantum chromodynamics (QCD), 3-jet events are produced in e^+e^- annihilation when either the primary quark or primary anti-quark emits a hard gluon ($e^+e^- \rightarrow q\bar{q}g$). Several groups^{1,2} have used these 3-jet ($q\bar{q}g$) events to study the impact of hard gluon bremsstrahlung on the hadronization process. One of the effects which they have observed, often referred to as the string effect³, is a depletion of particles in the angular region between the quark and anti-quark jets relative to the numbers of particles in the regions between the quark and gluon jets and the anti-quark and gluon jets. Recent QCD calculations⁴ attribute the string effect to coherence of the soft gluon emission from the $q\bar{q}g$ system. Soft gluons between the parent partons can be thought of as being produced by “color dipoles” which stretch between the quark, anti-quark, and gluon. Destructive interference of the radiation from the dipoles causes fewer particles to be produced in the region between the q and \bar{q} than would be expected without coherence. This behavior is predicted by the Lund “string” model³ of hadronic event production and by the Webber-Marchesini QCD shower model⁵, both of which account for the destructive interference in the region between the q and \bar{q} in a natural way. Independent fragmentation models^{6,7} cannot account for global effects such as this, and do not exhibit the string effect.

In this letter we present a new method of observing the string effect which relies on a detailed comparison of 3-jet events and radiative 2-jet events ($e^+e^- \rightarrow q\bar{q}\gamma$). The systematic errors due to event selection and jet finding are nearly identical for the two event types because they have very similar kinematics and topologies. Since the hard gluons of 3-jet ($q\bar{q}g$) events are replaced by photons, radiative 2-jet ($q\bar{q}\gamma$) events have only one color dipole, which lies in the angular region between the q and \bar{q} .⁴ Particle production in such events should therefore not be suppressed in this region. We observe the effects of the different color flows in $q\bar{q}g$ and $q\bar{q}\gamma$ events by comparing the azimuthal distributions of particles in their event planes.

For this measurement we use a data sample collected with the Mark II detector on the PEP e^+e^- storage ring at SLAC. The total integrated luminosity of 215 pb^{-1} ,

taken at a center of mass energy (E_{cm}) of 29 GeV, corresponds to approximately 90,000 hadronic events. Previous publications⁸ contain detailed descriptions of the Mark II detector, and we review here the features relevant to this analysis. Charged particle tracking is provided by inner and central drift chambers which have a combined momentum resolution of $(\delta p/p)^2 = (0.025)^2 + (0.01p)^2$ (p is the particle momentum in GeV/c). A lead-liquid-argon electromagnetic calorimeter is used to detect photons. The calorimeter is 14 radiation lengths thick, covers 64% of 4π in the central region, and has an energy resolution of $\delta E/E = 0.14/\sqrt{E}$ (E in GeV).

Charged tracks used in this analysis are required to have at least 100 MeV/c of momentum in the plane transverse to the beam axis and to have $|\cos\theta| \leq 0.8$ with respect to this axis. The track's closest approach to the beam interaction point must be within 10 cm in z and 5 cm in r (r is measured in the x - y plane). For tracks with momenta less than 1 GeV/c, the cut on r is loosened to $r \cdot p \leq 5$ cm GeV/c to account for multiple scattering errors. Photons included in this analysis must deposit at least 250 MeV in the liquid-argon calorimeter and be farther than 7 cm (at the radius of the calorimeter) from the closest charged track.

To obtain a clean sample of hadronic events, we require an event to have at least 5 charged tracks and a detected total energy (charged + neutral) $E_{vis} \geq 0.25E_{cm}$. The event's reconstructed primary vertex must be within 5 cm of the beam spot in the x - y plane, and within 10 cm in z . Its thrust axis must satisfy $|\cos\theta| \leq 0.7$. After applying these cuts, we obtain 73,477 events.

We select 3-jet candidates from hadronic events without radiative photon candidates (defined below). The Lund cluster algorithm⁹ is used to find candidate events with three clusters (jets) of particles. If \hat{n}_i is the normalized direction vector for jet i , we require $|\hat{n}_1 \cdot (\hat{n}_2 \times \hat{n}_3)| \leq 0.34$ to insure that the events are planar. We define an event plane using the thrust tensor¹⁰, and project the jet direction vectors into this plane. Jet energies are calculated from the angles between the projected direction vectors¹¹, and the jets are labelled according to their energy E_i with

jet 1 the most energetic and jet 3 the least energetic. We require $E_1 \leq 0.98E_{beam}$ ($E_{beam} = \frac{1}{2}E_{cm}$) to reduce the 2-parton background, and $E_3 \geq 3.0$ GeV for reasons discussed below. After all cuts, 6585 3-jet events remain. To aid in the study of backgrounds and systematic errors, we have produced a large sample of Monte Carlo events using the Lund hadronic event generator³ and a detailed simulation of the Mark II detector. First-order initial state radiative processes are included in the Lund generator.¹² From these events, we estimate that 1% of the selected 3-jet events are misidentified 2-parton events¹³, and that jets 1, 2, and 3 are produced by the gluon 9%, 25%, and 65% of the time, respectively.

Radiative 2-jet events are selected from hadronic events with a radiative photon candidate of measured energy $E_\gamma \geq 2.5$ GeV. Since a true radiative photon with this much energy would be well separated from any hadronic jets in the event, we require that there be no moderately energetic ($p \geq 500$ MeV/c) charged tracks within a 30° cone around the candidate photon. If more than one photon in a given event passes these cuts, we choose the one with the highest energy. There are 3474 events with candidate photons.

We then apply the Lund cluster algorithm to events with photon candidates. All tracks are used in the cluster search except this photon. We retain 2-cluster events, and include the photon as a third "jet." The resulting events are then treated like the 3-jet events discussed earlier in that they are required to be planar, the jet energies $E_1 > E_2 > E_3$ are calculated using the angles between the projections of the jets in the event plane, and the same cuts on E_1 and E_3 are applied. Because we require radiative photons to deposit at least 2.5 GeV in the calorimeter, the cut on E_3 assures similar kinematics in the two event samples. Finally, to insure that the photon energy measured in the calorimeter ($E_\gamma^{(LA)}$) is consistent with its energy calculated from the angles between the jets ($E_\gamma^{(angles)}$), we require $|\Delta_\gamma| \leq 0.3$, where

$$\Delta_\gamma \equiv \frac{E_\gamma^{(LA)} - E_\gamma^{(angles)}}{E_{beam}} .$$

There are 544 radiative events that pass all cuts. With our Monte Carlo sample, we

estimate that 15% of these are events with a misidentified π^0 , which is the primary source of background. The photon is jet 1, 2, or 3 with a frequency of 17%, 24%, or 59%, respectively.

For each of the jets in the selected $q\bar{q}\gamma$ and $q\bar{q}g$ events, an event plane angle ϕ is measured relative to the projection of jet 1, with the direction of increasing ϕ toward jet 2. By definition, then, jet 1 has $\phi = 0$ and jet 2 has a smaller value of ϕ than jet 3. The average jet energies ($\langle E_1 \rangle$, $\langle E_2 \rangle$, and $\langle E_3 \rangle$) and event plane angles ($\langle \phi_1 \rangle$, $\langle \phi_2 \rangle$, and $\langle \phi_3 \rangle$) for the selected $q\bar{q}\gamma$ and $q\bar{q}g$ samples are in excellent agreement, typically differing by less than their statistical errors.

If a depletion of particles due to a string effect is present in $q\bar{q}g$ events, it should occur principally between jets 1 and 2 since jet 3 is the gluon jet 65% of the time. Therefore the $q\bar{q}\gamma$ events of interest are those in which the photon is jet 3. There are 320 such events. The azimuthal particle flows in the $q\bar{q}g$ and $q\bar{q}\gamma$ events are displayed in Fig. 1(a), where we plot

$$\rho(\phi) \equiv \frac{1}{N_{events}} \frac{dn_{tracks}}{d\phi},$$

the charged track density as a function of the event plane angle ϕ . The string effect should be enhanced for particles with large transverse masses $[(m)^2 + (p_{\perp}^{(out)})^2]^{1/2}$, where $p_{\perp}^{(out)}$ is the component of particle momentum perpendicular to the event plane.^{3,14} Figure 1(b) shows the charged track density for tracks with $|p_{\perp}^{(out)}| \geq 300$ MeV/c. In the angular region between $\phi = 0^\circ$ and $\phi = 150^\circ$, which separates the q and \bar{q} for all of the $q\bar{q}\gamma$ events and for 65% of the $q\bar{q}g$ events, the figures clearly show a depletion in the $q\bar{q}g$ data relative to the $q\bar{q}\gamma$ data, and this depletion is enhanced by the $p_{\perp}^{(out)}$ cut. We use the Lund model to investigate possible systematic errors in our analysis, and show its predictions for $\rho(\phi)$ in Fig. 1. It has previously been shown^{1,2} that independent fragmentation (IF) models do not exhibit the string effect, and as an additional check we have included in Fig. 1 the $\rho(\phi)$ distributions for $q\bar{q}g$ events selected from a sample of hadronic events generated¹⁵ with the Ali IF model.⁷

To reduce the possibility that systematic errors might result from different jet angular distributions in the two event samples, the charged particle density is also plotted (see Figs. 2(a) and 2(b)) relative to x_ϕ , a “normalized” ϕ^1 . The variable x_ϕ is defined for tracks between jets 1 and 2 as ϕ_t/ϕ_2 , where ϕ_t is the ϕ of the track, and ϕ_2 is the ϕ of jet 2. Figures 2(c) and 2(d) show the ratios of the charged track density distributions

$$r(x_\phi) \equiv \frac{\left[\frac{1}{N} \frac{dn}{dx_\phi} \right]_{q\bar{q}g}}{\left[\frac{1}{N} \frac{dn}{dx_\phi} \right]_{q\bar{q}\gamma}}$$

for all tracks and for tracks with $|p_\perp^{(out)}| \geq 300$ MeV/c. From our sample of Lund Monte Carlo events, we estimate that possible contributions to $r(x_\phi)$ from event selection and cluster finding biases are less than 5%. This estimate is supported by our Ali Monte Carlo sample, which predicts an $r(x_\phi)$ distribution that is similar to the data in statistical significance and is consistent with unity. After adding a 5% systematic error to the statistical errors shown in Fig. 2, the χ^2 statistic for the hypothesis that $r(x_\phi) = 1$ in Fig. 2(c) is 33.3 for 8 degrees of freedom. A similar calculation for Fig. 2(d) yields a χ^2 of 48.8, again for 8 degrees of freedom. Thus, a clear difference in hadron density in the angular region between the q and \bar{q} in $q\bar{q}g$ and $q\bar{q}\gamma$ events is demonstrated by the data, establishing that hard gluon bremsstrahlung has global effects on particle production in hadronic events.

In summary, we have found clear evidence for a depletion of particles between the q and \bar{q} jets in 3-jet events relative to the number present in radiative 2-jet events. Because these two kinds of events have similar overall particle flow distributions, accurate comparisons of the particle densities between the jets in the events are possible. As expected, the depletion is enhanced for tracks with large momentum components out of the event plane.

REFERENCES

1. W. Bartel *et al.*, Phys. Lett. **101B**, 129 (1981), and Phys. Lett. **134B**, 275 (1984).
2. H. Aihara *et al.*, Z. Phys. C **28**, 31 (1985); M. Althoff *et al.*, Z. Phys. C **29**, 29 (1985).
3. B. Andersson, G. Gustafson, G. Ingelman and T. Sjöstrand, Phys. Rep. **97**, 33 (1983).
4. Ya. I. Azimov, Yu. L. Dokshitzer, V. A. Khoze, and S. I. Troyan, Phys. Lett. **165B**, 147 (1985).
5. G. Marchesini and B. R. Webber, Nucl. Phys. B **238**, 1 (1984); B. R. Webber, Nucl. Phys. B **238**, 492 (1984).
6. P. Hoyer *et al.*, Nucl. Phys. B **161**, 349 (1979)
7. A. Ali, E. Pietarinen, G. Kramer, and J. Willrodt, Phys. Lett. **93B**, 155 (1980).
8. R. H. Schindler *et al.*, Phys. Rev. D **24**, 78 (1981); G. S. Abrams *et al.*, IEEE Trans. Nucl. Sci. **27**, 59 (1980).
9. T. Sjöstrand, Computer Phys. Comm. **39**, 347 (1986); A. Bäcker, Z. Phys. C **12**, 161 (1982).
10. The eigenvectors of the thrust tensor are found in the following manner: We define \hat{e}_1 to be the standard thrust axis. A "thrust axis" is then found in the plane perpendicular to \hat{e}_1 ; this axis is \hat{e}_2 . The final vector \hat{e}_3 is defined by $\hat{e}_3 = \hat{e}_1 \times \hat{e}_2$.
11. The jet energies are calculated using

$$E_i = \frac{2 E_{beam} \beta_j \beta_k \sin \theta_i}{\beta_2 \beta_3 \sin \theta_1 + \beta_1 \beta_3 \sin \theta_2 + \beta_1 \beta_2 \sin \theta_3} ,$$

where i, j , and k are cyclic and θ_i is the angle between jets j and k . For the photon jet in $q\bar{q}\gamma$ events, $\beta = 1$. Otherwise, a jet's β is calculated assuming $M_i = \alpha E_i$. For 3-jet events, this assumption reduces the above equation to its more common form (one without the β 's). Although we use $\alpha = 0.45$ for

this analysis, our results are insensitive to values in the range $0.0 \leq \alpha \leq 0.7$.

12. F. A. Berends, R. Kleiss, and S. Jadach, Nucl. Phys. B **203**, 63, (1982), and Computer Phys. Comm. **29**, 185 (1983).
13. We used a y_{min} cut of 0.015 in our version of the Lund generator. The value of y_{min} determines where the differential cross-sections are cut off in calculating the 3-parton and 4-parton matrix elements. In our sample of Lund Monte Carlo events, 20% are 2-parton events, 70% are 3-parton events, and 10% are 4-parton events.
14. J. Randa, Phys. Rev. Lett. **43**, 602 (1979); I. Montvay, Phys. Lett. **84B**, 331 (1979).
15. The Monte Carlo program we used to generate our sample of Ali Monte Carlo events included first order initial state radiative processes and a simulation of the Mark II detector.

FIGURE CAPTIONS

1. The charged track density as a function of the event plane angle ϕ . The angular region between $\phi = 0^\circ$ and $\phi = 150^\circ$ separates the q and \bar{q} for all of the $q\bar{q}\gamma$ events and for 65% of the $q\bar{q}g$ events.
2. The charged track density in the region between jets 1 and 2 versus the normalized angle x_ϕ . The densities for $q\bar{q}g$ and $q\bar{q}\gamma$ events are displayed in (a) and (b), and the ratios of their densities are shown in (c) and (d). The bin width in the plots is 0.125.

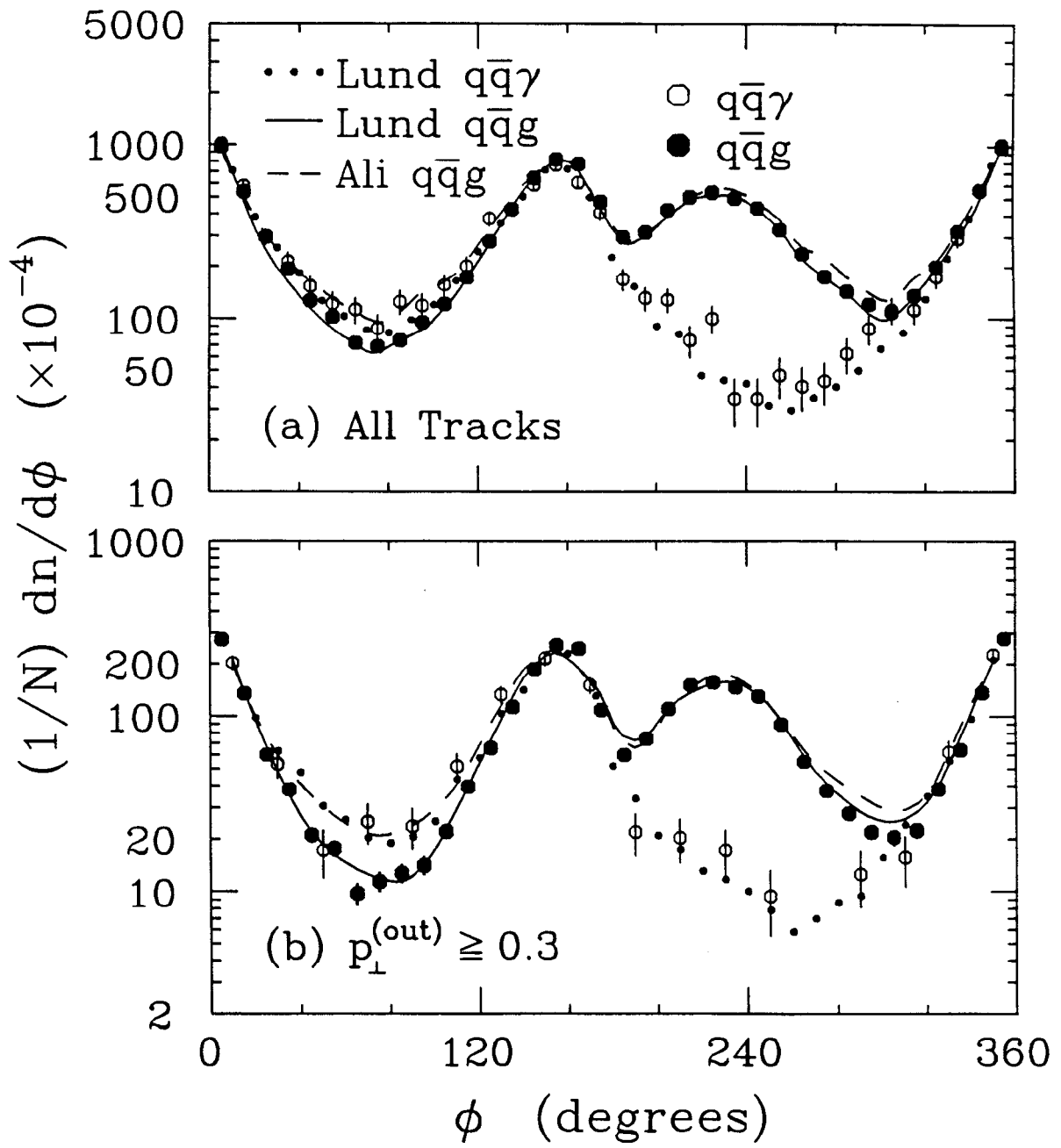


Fig. 1

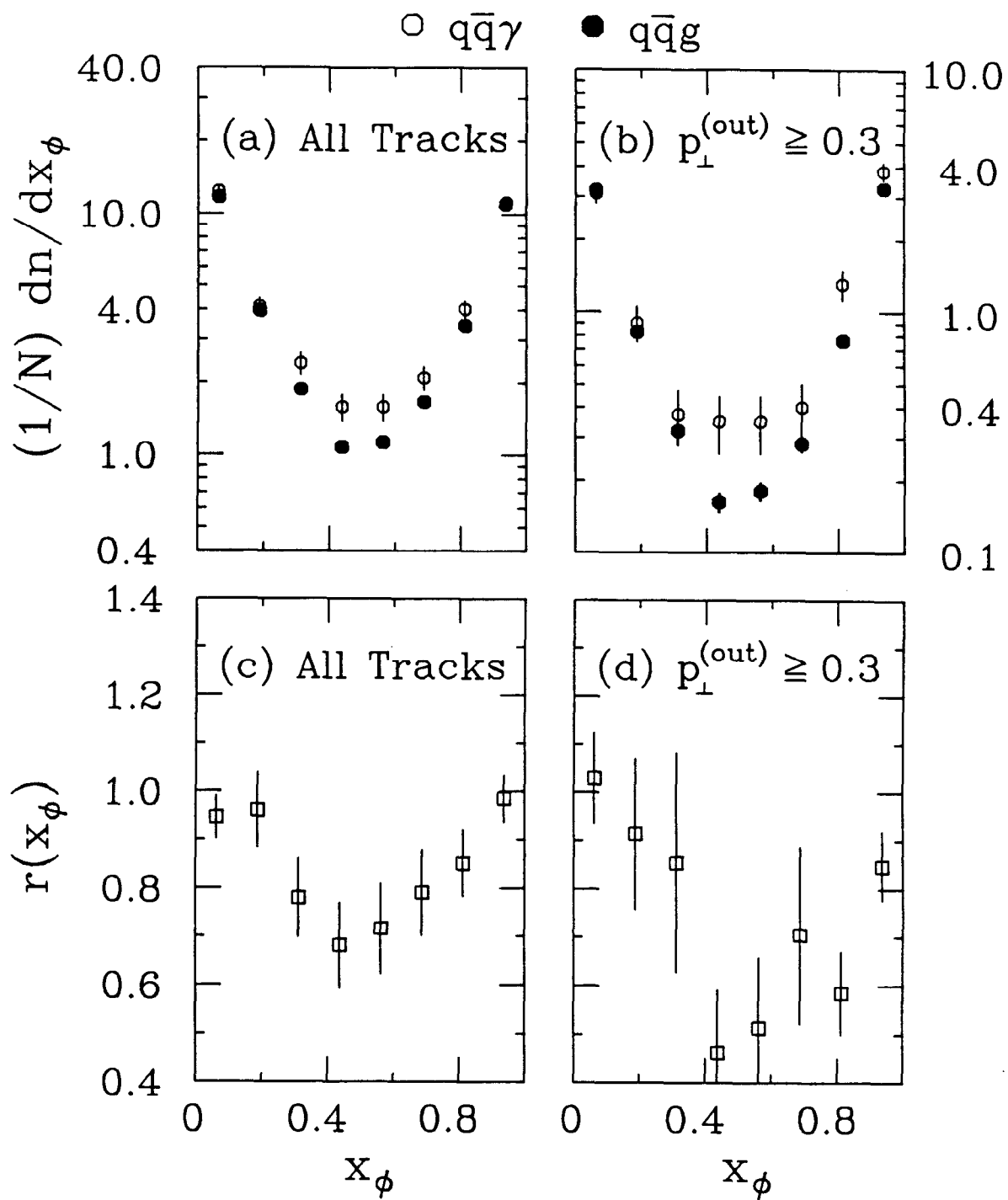


Fig. 2